

Fluorine-induced J-aggregation enhances emissive properties of a new NLO push–pull chromophore†

Cite this: *J. Mater. Chem. C*, 2014, 2, 5275Received 1st April 2014
Accepted 29th April 2014

DOI: 10.1039/c4tc00665h

www.rsc.org/MaterialsC

Chiara Botta,^{*a} Elena Cariati,^{*b} Gabriella Cavallo,^c Valentina Dichiarante,^c Alessandra Forni,^{*d} Pierangelo Metrangolo,^{*c} Tullio Pilati,^c Giuseppe Resnati,^{*c} Stefania Righetto,^b Giancarlo Terraneo^c and Elisa Tordin^b

A new fluorinated push–pull chromophore with good second-order NLO properties even in concentrated solution shows solid state intermolecular aryl–fluoroaryl interactions leading to J-aggregates with intense solid state luminescence.

Over the last few decades, organic-based optoelectronic materials displaying good 2nd order nonlinear optical (NLO) and emission properties have received great scientific attention.¹ Among all possible substrates, linear π -conjugated organic molecules, and notably *p*-phenylene vinylene (PPV) derivatives, are of particular interest due to their broad absorption bands, high luminescence quantum yields, and large Stokes shifts.² Moreover, PPV structures have been used as convenient π -bridges between strong electron donor (D) and acceptor (A) groups, whose electronic properties can be finely tuned by the insertion of suitable electron-withdrawing or donating substituents. In this respect, fluorination of A groups offers the possibility of modulating optical and electrical properties of push–pull organic chromophores, lowering their HOMO and LUMO energy levels and facilitating the charge transfer process,³ thus enhancing the 2nd order NLO response.⁴ Fluorination also affects crystal packing of conjugated organic materials,⁵ which is a key issue in determining their electronic and optical properties,⁶ and therefore their potential use in electronic and optoelectronic devices.⁷

On the other hand, linear π -conjugated materials tend to strongly aggregate in the solid state and in concentrated solutions, yielding π -stacked structures, which often suppress luminescence and NLO properties. A good strategy to optimize both properties is to design molecules characterized by a low tendency to aggregate when dispersed or dissolved, but self-assemble into J-type aggregates in the solid state. J-aggregates are characterized by a narrow and intense absorption band, bathochromically shifted with respect to the isolated molecule, and are known to enhance both the emissive⁸ and the NLO properties.⁹

Aryl–fluoroaryl interactions,¹⁰ among others,¹¹ have been exploited to dictate self-assembly of large aromatic chromophores into J-aggregates.^{12,13}

We have recently reported the synthesis, structural, and optical characterization of a new NLO chromophore consisting of a push–pull system where a PPV moiety spaces an electron-donor end, working as the halogen-bond-acceptor terminus, and a *p*-iodotetrafluorophenyl end, working as the halogen-bond-donor terminus (**1a** in Scheme 1).¹⁴ This chromophore, while being effective from the point of view of NLO properties, did not show any emission in the solid state and a very low one in solution (Quantum Yield, QY = 0.14 in toluene), as a likely consequence of the presence of iodine. Here our attention focuses on the de-iodinated derivative **1b** (Scheme 1), which being devoid of the I atom, should not only be preserved from the heavy atom effect on luminescence, but also favor the aryl–fluoroaryl interactions with respect to self-complementary halogen bonded arrangements. This, in fact, results in J-aggregates in the solid state due to antiparallel stacking of (2,3,5,6-tetrafluorostyryl)benzene moieties. As a consequence of this, **1b** shows an intense solid state luminescence. Moreover, due to its low tendency to aggregate in solution, it shows a large NLO response even at high concentrations.

Standard synthetic procedures and flash chromatography purification afforded **1b** in high yield as bright yellow powder, which was fully characterized by ¹H and ¹⁹F solution-NMR, FT-IR, mass spectrometry and dynamic light scattering (DLS)

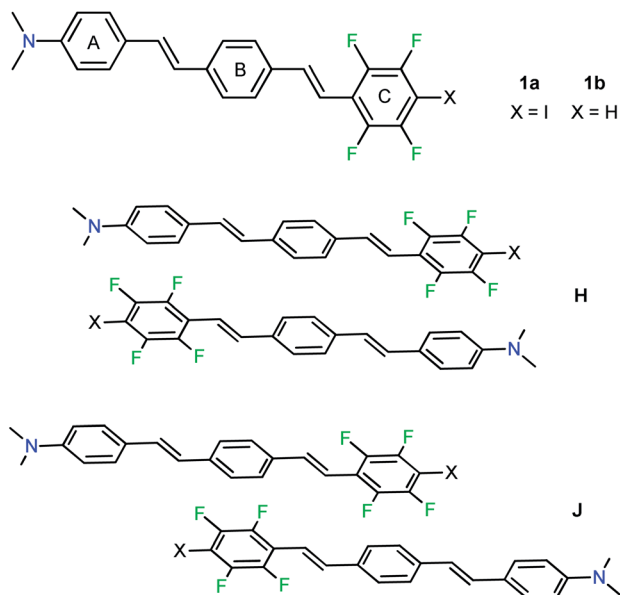
^aISMAL-CNR, via Bassini 15, 20133 Milan, Italy. E-mail: chiara.botta@ismal.cnr.it; Fax: +39 02 7063 6400; Tel: +39 02 2369 9734

^bDept. Chemistry and INSTM UDR Milano, University of Milan, via Golgi 19, I-20133 Milan, Italy. E-mail: elena.cariati@unimi.it; Fax: +39 02 5031 4405; Tel: +39 02 5031 4370

^cNFMLab, DCMIC, Politecnico di Milano, via Mancinelli 7, 20131 Milan, Italy. E-mail: pierangelo.metrangolo@polimi.it; giuseppe.resnati@polimi.it; Fax: +39 02 2399 3180; Tel: +39 02 2399 3041; +39 02 2399 3032

^dISTM-CNR, University of Milan, via Golgi 19, I-20133 Milan, Italy. E-mail: alessandra.forni@istm.cnr.it; Fax: +39 02 5031 4300; Tel: +39 02 5031 4273

† Electronic supplementary information (ESI) available: All experimental details as well as CIF. CCDC 961738. For ESI and crystallographic data in CIF or other electronic format see DOI: 10.1039/c4tc00665h



Scheme 1 Molecular structure of 4-(*N,N*-dimethylamino)-4'-(2,3,5,6-tetrafluorostyryl)-stilbene (**1b**) and its iodinated derivative **1a**.

measurements. **1b** was also subjected to full optical characterization in solution and in the solid state, and to single crystal X-ray analysis.

The absorption spectrum of **1b** in solution (Fig. S1†) showed a weak solvatochromic effect, whereas a large emission red-shift occurred when increasing solvent polarity, with photoluminescence (PL) maximum moving from 445 nm in pentane to 604 nm in acetonitrile. The PL quantum yield of **1b** was 0.90 in toluene, close to that previously reported for a similar PPV derivative.¹⁵

Second-order NLO properties of **1b** were examined by the solution-phase electric field induced second-harmonic (EFISH) generation method. Measurements of $\mu\beta_\lambda$ (the product between the molecular dipole moment μ and the projection of the quadratic hyperpolarizability tensor β_{tot} along μ) were carried out in CHCl_3 and DMF solutions, at 1907 nm non-resonant wavelength, giving all large and positive values (Table 1). Such values, very close to those measured in CHCl_3 for the *p*-iodotetrafluorophenyl analogue **1a**,¹⁴ can be explained by a high difference in the dipole moment from the ground to the excited state ($\Delta\mu_{12}$). For compound **1b**, TD-PBE0/6-311++G(d,p) calculations *in vacuo*¹⁶ provided a $\Delta\mu_{12}$ value of 17.7 D, slightly lower than that computed for **1a**, 19.0 D, at the same level of theory (see Table S1† for a detailed comparison between computed properties of compounds **1a** and **1b**). Interestingly, unlike other D-PPV-A systems,¹⁵ which show strong concentration

quenching of NLO properties and strong solvent dependence, the $\mu\beta_\lambda$ value of **1b** in CHCl_3 solutions did not change on going from 10^{-3} to 10^{-4} M. This behaviour can be rationalized on the basis of the poor tendency of **1b** to form aggregates in solution at concentrations up to 10^{-3} M as demonstrated by both DLS and ^{19}F NMR measurements at different concentrations. In fact, no shift was detected in ^{19}F signals and no aggregates were observed using DLS, proving the absence of significant intermolecular interactions in solution. This result is particularly relevant to the idea of device construction since a limiting factor is often represented by dye loading.

Furthermore, the $\mu\beta_\lambda$ value of **1b** did not increase or change sign on going from CHCl_3 to DMF, as was observed for **1a**, as a consequence of the specific involvement of the iodine atom in the formation of a halogen bond with the oxygen atom of DMF.^{14,14} In the case of **1b**, the insensitivity of $\mu\beta_\lambda$ to the environment indicates the absence of a specific attractive interaction involving the *p*-hydrogen atom of the fluorinated ring and affecting the NLO response.

Single crystals of **1b**, obtained upon slow evaporation at r.t. of a chloroform solution, consisted of extremely thin and friable millimetric yellow plates with micrometric thickness (see ESI† for details concerning the experimental setup, structure solution, refinement, and full description). The (001) one being the only developed face, these crystals can be considered almost “two-dimensional”, with a high tendency to curl up. As far as the supramolecular organization of the molecules of **1b** in the crystal is concerned, the packing is completely different from that of *p*-iodotetrafluorophenyl analogue **1a**, where halogen bonding drives the molecular self-assembly in the solid state giving rise to infinite chains. Here, the hydrogen atom on the fluorinated aromatic ring, despite its quite acidic properties, is not involved in any strong attractive interaction. Interestingly, the main structural feature is a π - π antiparallel overlapping of a pile of (tetrafluorostyryl)benzene groups, where the centroid of the fluorinated ring is located at 3.772 and 3.829 Å from the two nearest hydrogenated ones (see Fig. 1 showing, among others, the shortest C \cdots C intermolecular contacts, C12 \cdots C12 $_{-x,1-y,2-z}$, 3.326 Å, and C9 \cdots C5 $_{1-x,1-y,2-z}$, 3.379 Å). In such an arrangement, adjacent molecules are sufficiently slipped to give rise to J-aggregates (slip angles $\theta_1 = 20.76^\circ$ and $\theta_2 = 20.12^\circ$, Fig. S3†)^{8b} with optimized aryl-fluoroaryl face-to-face interactions. Moreover, these piles give rise to side-to-side F \cdots C_{Ar} contacts. The result is the formation of a 2D structure in the plane (001), from whose surface the dimethylamino-benzene groups emerge, parallel to the (201) direction. These deeply cut

Table 1 $\mu\beta_\lambda$ values ($\times 10^{-48}$ esu) of NLO-phore **1b** by EFISH

Concentration (M)	CHCl_3	DMF
10^{-3}	+800	+850
2×10^{-4}	+816	—

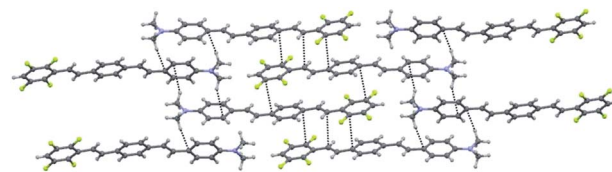


Fig. 1 A cluster of **1b** molecules projected down the crystallographic *b* axis, showing the shortest π - π and methyl $\cdots\pi$ interactions as dotted lines.

surfaces fit together due to a side-to-face coupling of two dimethylamino-benzene groups, the angle being about 64° between the two aromatic rings (see Fig. S6† in the ESI for an additional projection of the crystal packing evidencing the relative orientation of adjacent J-aggregates). This arrangement is promoted by attractive $\text{CH}\cdots\pi$ interactions between dimethylamino-benzene groups of adjacent J-aggregates (see in Fig. 1 contacts $\text{H23A}\cdots\text{C17}_{-x,y-1/2,3/2-z}$, 2.88 Å and $\text{H24A}\cdots\text{C18}_{-1-x,1/2+y,3/2-z}$, 2.85 Å).

Interestingly, pairs of molecules of **1b** did not fully overlap in the crystal in an antiparallel manner as could be expected from the optimized overlap of the opposite quadrupolar moments of the dimethylamino- and tetrafluoro-benzene rings (arrangement **H** in Scheme 1). DFT calculations at B97D/6-31++G(d,p) level on **1b** dimers were therefore performed,¹⁶ considering different arrangements as starting points for geometry optimization, and found three dimers with significant interaction energy. As expected, the most stable one, associated with a counterpoise-corrected interaction energy ΔE_{CP} of -23.6 kcal mol⁻¹, was the one with the two molecules fully overlapped according to arrangement **H**. In the other two, molecules were only partially overlapped and arranged either in an antiparallel (arrangement **J**, Scheme 1) or parallel fashion ($\Delta E_{\text{CP}} = -18.8$ and -17.4 kcal mol⁻¹, respectively). The antiparallel partially overlapped optimized geometry **J** reproduces quite well that observed in the crystal (see Fig. S7†). The tendency of **1b** to crystallize forming J-aggregates, instead of the most stable arrangement **H**, may find explanation in neglecting, in DFT calculations, of the additional intermolecular interactions, in particular the above-mentioned $\text{CH}\cdots\pi$ interactions between overlapping dimethylamino-benzene groups of adjacent J-aggregates, which could not take place in a hypothetical H-aggregate.

As far as solid-state PL properties of **1b** are concerned, native powders coming from chromatography purification displayed bright, narrow yellow emission centred at 524 nm, with a small Stokes shift (160 meV) and a PL QY of 0.70 (Fig. 2). Conversely,

powders of **1b** obtained by fast precipitation showed broader emission with a shoulder at about 565 nm, and 0.36 PL QY. The electronic absorption spectrum of both powders in nujol mull showed the superposition of two bands (see Fig. S2 in the ESI†), a broad and strong band centred at around 403 nm, resembling that in solution, and a strong, red-shifted peak at 476 nm. The latter is the typical feature of J-aggregates in the solid state, which agrees with the single crystal X-ray analysis. In order to assess the molecular-level PL properties of **1b**, we prepared its inclusion complex with deoxycholic acid (DCA), which is known to prevent solid-state aggregation.¹⁷ As shown in the inset of Fig. 2, emission of the **1b**-DCA adduct is blue-shifted to 511 nm, with QY = 0.72 and a Stokes shift of about 480 meV. Interestingly, PL QY of native **1b** is comparable to that of **1b**-DCA, whereas its Stokes shift is much smaller. However, the origin of the broader and weaker emission of the fast precipitated powder would require further analysis.

The quite different PL properties of the two powder samples would suggest different crystallinity and packing interactions for the two samples shown in Fig. 2. Unexpectedly, XRPD spectra (Fig. 3) show the same diffraction pattern for both samples, the only difference being the average size of the crystallites, smaller for the fast precipitated powders than for the native ones (56 and 134 nm respectively, see ESI†).

In order to assess the influence of crystal size on the PL properties of **1b**, we have mechanically milled **1b** to further reduce the crystallite average size (see Fig. S5†). Even though the crystallinity of the powders is not affected by grinding (XRPD spectra show the same diffraction pattern, see Fig. 3), the room temperature PL spectrum displays a relevant (197 meV) red shift after grinding (see Fig. 4, left) accompanied by a sensitive reduction of the PL QY (by a factor 4). However, by lowering the temperature, the PL spectra of the two powders show the same peaks, with a different relative intensity distribution (see Fig. 4, right).¹⁸

At room temperature, exciton migration induces trapping at lower energy centres (contaminations or structural dislocations

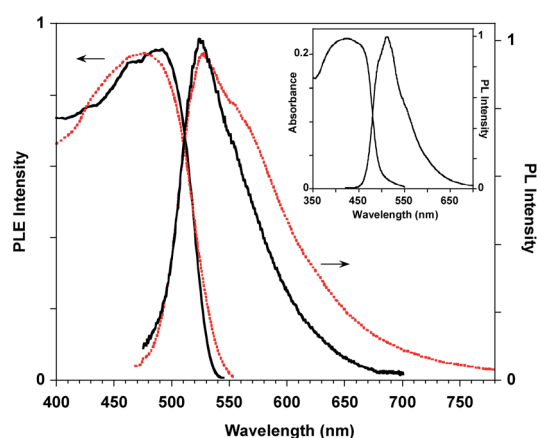


Fig. 2 Solid state PL excitation (PLE) and emission spectra of powders of **1b** from chromatography purification (black line) and from fast precipitation (red dashed line). Inset: absorption and emission spectra of the **1b**-DCA inclusion complex.

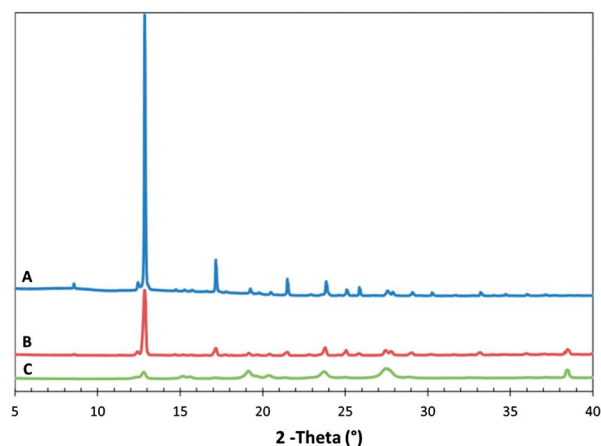


Fig. 3 XRPD patterns of **1b**: (A) native powder; (B) powder obtained by fast precipitation; (C) ball-milled powder. The crystallite average sizes were estimated through the Scherrer equation integrating the area underneath the XRD peak at $2\theta = 12.84^\circ$. The crystallite average sizes were 134, 56 and 34 nm for A, B and C, respectively.

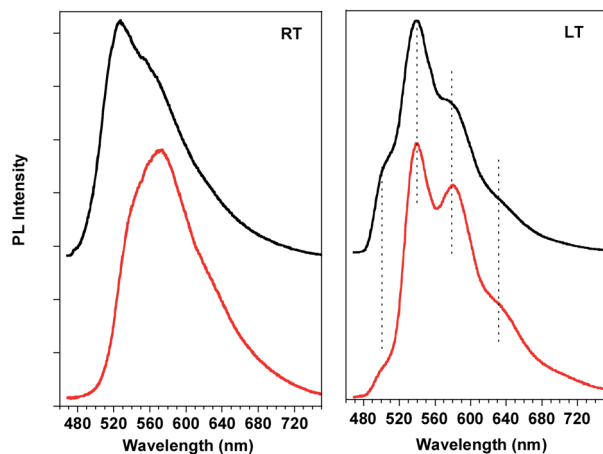


Fig. 4 PL spectra at room temperature (left) and at 80 K (right) of **1b** from fast precipitation before (top) and after (bottom) grinding. Spectra are shifted vertically for clarity and dotted lines are a guide for the eye.

located at the crystal grain boundaries) possessing lower emission efficiency.¹⁹ At low temperature the excitations are more localized and their migration towards the low energy trap states is hampered. The PL red-shift and lower QY observed for ground powders, at room temperature, can be accounted for by the higher content of low emissive traps, rather than to different crystal packing properties.

In conclusion, this study provides a new highly emissive push-pull NLO chromophore, whose solid-state molecular packing is driven towards J-type aggregation by means of aryl-fluoroaryl interactions. The absence of concentration quenching of the NLO properties is particularly relevant. In fact, for example, while electric poling of composite polymeric films with embedded molecular second-order NLO chromophores⁸ is an intensively investigated approach, it is often limited by the maximum loading of the dye inside the polymeric matrix.²⁰

The results described in this paper may pave the way to new design principles for the optimization of solid-state linear and NLO properties of organic chromophores. Moreover, we have shown that **1b** possesses interesting mechanofluorochromic properties²¹ with emission dependent on the powder average crystal sizes that can be tuned by grinding.

The mechanofluorochromic properties of **1b** as well as fabrication of optoelectronic devices thereof are under current investigation and will be reported elsewhere.

P. M. and G. T. thank the MIUR for financial support through the project 2010CX2TLM "InfoChem" (PRIN 2010–2011). A. F. and G. R. thank the MIUR for financial support through the project no. 2010ERFKXL (PRIN 2010–2011). A. F. acknowledges CINECA award no. HP10BFJG1H "IscrB-HEChro" 2011 for the availability of high performance computing resources.

Notes and references

- 1 S. P. Anthony, *ChemPlusChem*, 2012, **77**, 518; H. Dong, H. Zhu, Q. Meng, X. Gong and W. Hu, *Chem. Soc. Rev.*, 2012, **41**, 1754.

- 2 J. Gierschner and D. Oelkrug, *Encyclopedia of Nanoscience and Nanotechnology*, ed. H. S. Nalwa, 2004, vol. 8, p. 219; A. de Cuendias, R. C. Hiorns, E. Cloutet, L. Vignau and H. Cramail, *Polym. Int.*, 2010, **59**, 1452; J. Gierschner and S. Y. Park, *J. Mater. Chem. C*, 2013, **1**, 5818–5832.
- 3 C. Martinelli, G. M. Farinola, V. Pinto and A. Cardone, *Materials*, 2013, **6**, 1205.
- 4 A. Papagni, S. Maiorana, P. Del Buttero, D. Perdicchia, F. Cariati, E. Cariati and W. Marcolli, *Eur. J. Org. Chem.*, 2002, 1380; P. Romaniello and F. Lelj, *J. Fluorine Chem.*, 2004, **125**, 145.
- 5 R. Berger, G. Resnati, P. Metrangolo, E. Weber and J. Hulliger, *Chem. Soc. Rev.*, 2011, **40**, 3496.
- 6 P. S. Salini, M. G. Derry Holaday, M. L. P. Reddy, C. H. Suresh and A. Srinivasan, *Chem. Commun.*, 2013, **49**, 2213.
- 7 S. Varghese and S. Das, *J. Phys. Chem. Lett.*, 2011, **2**, 863.
- 8 (a) E. E. Jelley, *Nature*, 1936, **138**, 1009; (b) F. Wurthner, T. E. Kaiser and C. R. Saha-Moller, *Angew. Chem., Int. Ed.*, 2011, **50**, 3376.
- 9 F. Nunzi, S. Fantacci, F. De Angelis, A. Sgamellotti, E. Cariati, R. Ugo and P. Macchi, *J. Phys. Chem. C*, 2008, **112**, 1213.
- 10 C. Dai, P. Nguyen, T. B. Marder, A. J. Scott, W. Clegg and C. Viney, *Chem. Commun.*, 1999, 2493; S. W. Watt, C. Dai, A. J. Scott, J. M. Burke, R. L. Thomas, J. C. Collings, C. Viney, W. Clegg and T. B. Marder, *Angew. Chem., Int. Ed.*, 2004, **43**, 3061; J. C. Collings, A. S. Batsanov, J. A. K. Howard, D. A. Dickie, J. A. C. Clyburne, H. A. Jenkins and T. B. Marder, *J. Fluorine Chem.*, 2005, **126**, 515.
- 11 K. Reichenbacher, H. I. Süss and J. Hulliger, *Chem. Soc. Rev.*, 2005, **34**, 22; S. Yagai, *J. Photochem. Photobiol., C*, 2006, **7**, 164; E. Cariati, A. Forni, S. Biella, P. Metrangolo, F. Meyer, G. Resnati, S. Righetto, E. Tordin and R. Ugo, *Chem. Commun.*, 2007, 2590.
- 12 W. J. Feast, P. W. Lövenich, H. Puschmann and C. Taliani, *Chem. Commun.*, 2001, 505; R. Capelli, M. A. Loi, C. Taliani, H. B. Hansen, M. Murgia, G. Ruani, M. Muccini, P. W. Lövenich and W. J. Feast, *Synth. Met.*, 2003, **139**, 909.
- 13 S. S. Babu, V. K. Praveen, S. Prasanthkumar and A. Ajayaghosh, *Chem.–Eur. J.*, 2008, **14**, 9577; D. Yan, A. Delori, G. O. Lloyd, T. Friščić, G. M. Day, W. Jones, J. Lu, M. Wei, D. G. Evans and X. Duan, *Angew. Chem., Int. Ed.*, 2011, **50**, 12483.
- 14 E. Cariati, G. Cavallo, A. Forni, G. Leem, P. Metrangolo, F. Meyer, T. Pilati, G. Resnati, S. Righetto, G. Terraneo and E. Tordin, *Cryst. Growth Des.*, 2011, **11**, 5642.
- 15 C. Coluccini, A. K. Sharma, M. Caricato, A. Sironi, E. Cariati, S. Righetto, E. Tordin, C. Botta, A. Forni and D. Pasini, *Phys. Chem. Chem. Phys.*, 2013, **15**, 1666.
- 16 M. J. Frisch, *et al.*, *Gaussian 09, Revision C.01*, Gaussian, Inc., Wallingford CT, 2011.
- 17 C. Botta, P. Betti and M. Pasini, *J. Mater. Chem. A*, 2013, **1**, 510; G. Bongiovanni, C. Botta, G. Di Silvestro, A. Mura and R. Tubino, *Phys. Lett. A*, 1995, **208**, 165.

- 18 The different relative intensities of the vibronic peaks cannot be due to re-absorption processes since opposite behaviour would be expected in that case.
- 19 J. Gierschner, L. Lüer, B. Milián-Medina, D. Oelkrug and H. J. Egelhaaf, *J. Phys. Chem. Lett.*, 2013, **4**, 2686.
- 20 R. Macchi, E. Cariati, D. Marinotto, E. Tordin, R. Ugo, G. Santoro, M. C. Ubaldi, S. M. Pietralunga and G. Mattei, *J. Mater. Chem.*, 2011, **21**, 9778.
- 21 R. Gawinecki, G. Viscardi, E. Barni and M. A. Hanna, *Dyes Pigm.*, 1993, **23**, 73; P. L. Gentili, M. Nocchetti, C. Miliani and G. Favaro, *New J. Chem.*, 2004, **28**, 379; N. Fridman, S. Speiser and M. Kaftory, *Cryst. Growth Des.*, 2006, **6**, 1653; C. Weder, *Nature*, 2009, **459**, 45; Y. Sagara and T. Kato, *Nat. Chem.*, 2009, **1**, 605; Z. Chi, X. Zhang, B. Xu, X. Zhou, C. Ma, Y. Zhang, S. Liu and J. Xu, *Chem. Soc. Rev.*, 2012, **41**, 3878.